



Long-time global radiation for Central Europe derived from ISCCP Dx data

N. Petrenz, M. Sommer, F. H. Berger

► To cite this version:

N. Petrenz, M. Sommer, F. H. Berger. Long-time global radiation for Central Europe derived from ISCCP Dx data. Atmospheric Chemistry and Physics Discussions, 2007, 7 (3), pp.8333-8360. hal-00302872

HAL Id: hal-00302872

<https://hal.science/hal-00302872>

Submitted on 14 Jun 2007

HAL is a multi-disciplinary open access archive for the deposit and dissemination of scientific research documents, whether they are published or not. The documents may come from teaching and research institutions in France or abroad, or from public or private research centers.

L'archive ouverte pluridisciplinaire **HAL**, est destinée au dépôt et à la diffusion de documents scientifiques de niveau recherche, publiés ou non, émanant des établissements d'enseignement et de recherche français ou étrangers, des laboratoires publics ou privés.

**Long-time global
radiation derived
from ISCCP Dx data**

N. Petrenz et al.

Long-time global radiation for Central Europe derived from ISCCP Dx data

N. Petrenz¹, M. Sommer¹, and F. H. Berger^{1,2}

¹TU Dresden, Institute of Hydrology and Meteorology, Department of Meteorology, 01062 Dresden, Germany

²German Meteorological Service, Meteorological Observatory Lindenberg (FE LG), 15848 Tauche/Lindenberg, Germany

Received: 4 May 2007 – Accepted: 5 June 2007 – Published: 14 June 2007

Correspondence to: N. Petrenz (nadja.petrenz@forst.tu-dresden.de)

Title Page

Abstract

Introduction

Conclusions

References

Tables

Figures

◀

▶

◀

▶

Back

Close

Full Screen / Esc

Printer-friendly Version

Interactive Discussion

Abstract

The global Dx dataset of the “International Satellite Cloud Climatology Project” (ISCCP) with a spatial resolution of about $30 \times 30 \text{ km}^2$ was analysed to produce spatially highly resolved long-time datasets to describe the radiation budget for Central Europe over the period of 1984–2000. The computation of shortwave and longwave radiant flux densities at top of atmosphere and at surface was based on 1-D radiative transfer simulations. The simulations were carried out for all relevant atmospheric and surface conditions and the results were inserted into a look-up table. Thus, long-time calculations for all conditions and time slices of the Dx dataset could be realised. The study is focussed on the global radiation at surface.

The first examination was carried out for the ISCCP D1 and the ISCCP D2 dataset. These datasets, including cloud and surface information on a different spatial scale ($280 \times 280 \text{ km}^2$), were applied to the produced look-up table analogue to the Dx data. The calculated global radiation of the D1 and D2 dataset were compared to the Dx dataset. The differences between these datasets mainly range from $5\text{--}15 \text{ W m}^{-2}$ (2–6 %) with regional peaks up to 25 W m^{-2} (10 %).

The evaluation with the GEWEX “Surface Radiation Budget” (SRB) data emphasises differences between $5\text{--}25 \text{ W m}^{-2}$ (6–16%) over land areas. Deviations to an ISCCP provided flux data set vary from 0 W m^{-2} in the North up to 35 W m^{-2} (0–13%) in the South of Central Europe.

The global radiation datasets provided by the “Global Energy Balance Archive” (GEBA) and the “German Meteorological Service” (DWD) agree well, but they are $5\text{--}25 \text{ W m}^{-2}$ (7–10%) lower than the Dx results.

Annual analyses of global radiation of various regional climate models complete the study. It is figured out that the used models and methods reveal a couple of discrepancies. Especially in wintertime the results of our analysis differ to the considered models. Principally the uncertainties were caused by the determined range of values and simplifications for the computation of the radiative transfer simulation.

ACPD

7, 8333–8360, 2007

Long-time global radiation derived from ISCCP Dx data

N. Petrenz et al.

Title Page

Abstract

Introduction

Conclusions

References

Tables

Figures

◀

▶

◀

▶

Back

Close

Full Screen / Esc

Printer-friendly Version

Interactive Discussion

EGU

1 Introduction

The knowledge of incoming and outgoing shortwave and longwave radiant flux densities provides the key information for the net balance and thus for energy exchanges between atmosphere and surface. Therefore it is necessary to infer these radiant flux densities as accurately as possible to realise a correct characterisation of the Earth's climate system (Hollmann et al., 2006). The radiation budget is object of investigation in numerous studies, which infer radiant flux densities at top of atmosphere (TOA) and at surface using ground based measurements or remotely sensed data (Raschke et al., 2005, 2006).

Among others the “Global Energy Balance Archive” (GEBA/Gilgen et al., 1997; Gilgen and Ohmura, 1999), the “Baseline Surface Radiation Network” (BSRN/Ohmura et al., 1998), the “Atmospheric Radiation Measurement” (ARM/Stokes and Schwartz, 1994) or the “Surface Radiation Budget Network” (SURFRAD/Augustine et al., 2000) provide high quality datasets from surface observation sites with directly measured or derived radiant flux densities. Due to the point measurements spatial interpolations are ambiguous and mostly less representative because of the wide distances between the stations within meteorological networks. Remote sensing systems collect radiative properties and surface temperatures at different temporal and spatial scales allowing the derivation of area-integrated radiances and radiant flux densities at different atmospheric layers. In this regard the global datasets of the “Earth Radiation Budget Experiment” (ERBE/Barkstrom et al., 1989), the “International Satellite Cloud Climatology Project” (ISCCP/Schiffer and Rossow, 1983), the “Clouds and the Earth’s Radiant Energy System” (CERES/Wielicki et al., 1998) or the GEWEX “Surface Radiation Budget” (SRB/Stackhouse et al., 2000) are often applied. Estimations of shortwave and longwave surface radiation fluxes from satellite measurements are carried out with specially developed algorithms consisting of simple parameterisations concerning cloud physics, atmosphere and aerosols (Darnell et al., 1988, 1992; Gupta et al., 1992; Pinker and Laszlo, 1992; Pinker et al., 1995; Rossow and Zhang, 1995; Zhang et al., 1995). The

Long-time global radiation derived from ISCCP Dx data

N. Petrenz et al.

Title Page

Abstract

Introduction

Conclusions

References

Tables

Figures

◀

▶

◀

▶

Back

Close

Full Screen / Esc

Printer-friendly Version

Interactive Discussion

evaluation of calculated radiative flux components is complicated since the parameterisation of atmospheric and surface properties is still problematic in model approaches.

The decisive input to the climate system is the incoming solar radiation, which is nearly con-stant at TOA. Incoming solar radiation is attenuated by the atmosphere and the description of this process of radiative transfer is treated differently by the available transfer codes. Further investigations regarding other radiation budget components assume an exact determination of the direct and diffuse incoming solar radiation (global radiation). This paper describes and discusses a specially developed method for calculating radiation budget components at TOA and at surface using various ISCCP data. Detailed analyses and comparisons for the global radiation are shown.

2 Input data and method description

2.1 Data source

The ISCCP datasets with a current availability from July 1983 to December 2004 are used to compute the shortwave and longwave radiant flux components for both TOA and surface. At present three datasets (Dx/D1/D2) exist combining data of all available geostationary and polar orbit weather satellites (Rossow et al., 1996; Rossow and Schiffer, 1999). The datasets build up on each other (D1 on Dx and D2 on D1) and include a nearly complete global information of various cloud properties. Table 1 gives a summery of the spatial and temporal resolution of the datasets as well as the used parameters.

Additionally the weekly snow/ice cover data from the “NOAA/National Environmental Satellite Data and Information Service” (NESDIS) and from the NAVY/NOAA Joint Ice Center (see Rossow et al., 1991) are enclosed.

As reference the three-hourly ISCCP Dx data with a spatial sampling resolution of approx. $30 \times 30 \text{ km}^2$, one random pixel of 4–7 km without specific knowledge of location is characteristic for the whole grid cell, is used. ISCCP D1 and D2 are datasets with an

Title Page

Abstract

Introduction

Conclusions

References

Tables

Figures

◀

▶

◀

▶

Back

Close

Full Screen / Esc

Printer-friendly Version

Interactive Discussion

equal area grid of approx. $280 \times 280 \text{ km}^2$ ($2.5^\circ \times 2.5^\circ$ at the equator), but with different temporal sampling intervals. Thus the D1 dataset provides three-hourly cloud information and the D2 dataset is statistically averaged to three-hourly monthly means (see more details in Rossow et al., 1996).

All calculations are carried out over the period of 1984–2000 (17 years) covering a region of $65^\circ \text{ N}/35^\circ \text{ E}/30^\circ \text{ S}/15^\circ \text{ W}$ (henceforth Central Europe). In the run-up to radiative transfer simulations gaps, plausibility and spatial structures for each dataset are tested. The global D1 and D2 time series of cloud amount and surface temperature have only few gaps ($<0.2\%$). Due to the method creating the equal-area grid cells uncertainties in spatial structures are possible. But the analysis exhibited logical spatial structures. In contrast the gaps of parameters, which are estimated only during the day, like optical thickness, cloud type and reflectivity, are more extensive (approx. 5.0%) and cause uncertainties for further computations. Furthermore at the edge of the geostationary satellite images the data are either missing or of insufficient quality.

In Fig. 1d the mean global cloud amount of the D1 dataset over the whole period is shown in context with the calculated temporal trends. To avoid the influences of seasonal variations annual means are produced and applied to the trend analysis. A clear negative trend in the cloud amount of about 2.5% over wide areas with regional peaks of 15.0% and more is observed. To verify the detected trends the non-parametric Mann-Kendall test – applicable in case of non-linear trends – is used (Rapp, 2000):

$$Q = \frac{\sum_{i=1}^{N-1} \sum_{j=i+1}^N \text{sgn}(y_j - y_i)}{\sqrt{\frac{1}{18} [N(N-1)(2N+5)]}} \quad (1)$$

where Q is the numerical test value, N is the length of the time series, sgn describes the leading sign, y_i and y_j are the values to compare. The test only rates the relative increase or decrease of the values but provides no detailed information of time dependent changes. The corresponding confidence interval V and the probability value α

Long-time global radiation derived from ISCCP Dx data

N. Petrenz et al.

Title Page

Abstract

Introduction

Conclusions

References

Tables

Figures

◀

▶

◀

▶

Back

Close

Full Screen / Esc

Printer-friendly Version

Interactive Discussion

to every calculated Q are taken from Rapp (2000). In Fig. 1 the visible global trends are only significant within the contoured regions exhibiting a confidence interval of $V > 99.7\%$. At the edge of the geostationary satellite images the largest negative trends occur which are also statistically firmed. Evaluating these trends the time series of two joining pixel in two different areas are investi-gated (red circles).

Figure 1c reveals the inhomogenities over the period of August 1984 to December 1985 (black graph). Long-term measurement gaps of the operational geostationary satellite GOES-East were discovered that intensify these trends. The black graph in Fig. 1b represents a pixel that belongs to the disk recorded by the geostationary satellite INSAT. The data of this satellite only exist for the period of April 1988 to March 1989. Due to this huge failure only the data of polar orbit satellites were available twice per day therefore providing insufficient measurements. At the beginning of 1998 Meteosat-5 has been replaced to the position 63° East to compensate for the full disk of INSAT resulting in consistent time series. Regarding to these analyses the observed and assured trends within the critical regions are adulterated. For Central Europe only Meteosat data are used. There no profoundly long-term gaps and failures could be located.

The used ISCCP Dx dataset includes pixel level cloud information that is primarily based on the information of the cloud mask (1=clouds; 0=no clouds) and on relevant information of cloud top temperature, cloud top pressure and cloud optical thickness. With these parameters a classification of cloud classes and cloud layers according to Rossow et al. (1996) is carried out. 15 cloud classes and three cloud layers could be determined and the frequencies of each are calculated.

2.2 Radiative Transfer Model (RTM) and method

The computations are carried out with the complex 1-D RTM Streamer, that calculates radi-ances and radiant flux densities at each atmospheric level for several atmospheric and surface conditions (Key, 2001; version 3.0 beta 7). The solution of the radiative transfer equation can be realized for a horizontal plane-parallel atmosphere with the

Long-time global radiation derived from ISCCP Dx data

N. Petrenz et al.

Title Page

Abstract

Introduction

Conclusions

References

Tables

Figures

◀

▶

◀

▶

Back

Close

Full Screen / Esc

Printer-friendly Version

Interactive Discussion

Delta-2-Stream-Approximation (Toon et al., 1989) and the Discrete-Ordinate-Method (DISORT) according to Stamnes et al. (1988). To estimate shortwave ($0.2\text{--}4.0\ \mu\text{m}$) and longwave ($4.0\text{--}500.0\ \mu\text{m}$) radiant flux densities at different layers special input parameters are required regarding clouds, their geo-metrical, optical and microphysical properties as well as surface and atmospheric properties. First calculations are carried out for the monthly D2 dataset at 12:00 UTC. For that purpose the input parameters are taken directly from the dataset except information concerning the microphysics of clouds. The microphysical cloud parameters, like Liquid/Ice Water Content (LWC/IWC) and effective radius r_e , are defined according to Polar Radiation Fluxes from ISCCP (PRFI, 2000). Thus LWC is 0.2 gm^{-3} and r_e is $10\ \mu\text{m}$ for water clouds and IWC is 0.07 gm^{-3} and r_e is $30\ \mu\text{m}$ for ice clouds. Atmospheric and aerosol standard profiles from surface (0 km) up to TOA (100 km) are specified within the model. The different vegetation types of the D datasets are adapted to the vegetation types defined in the RTM Streamer followed by the internal modulation of reflectivity.

To handle radiative transfer computations for all ISCCP D datasets and all radiation budget components for the period of 1984–2000 (17 years) look-up tables are a useful instrument. Hence relevant nodes of all individual model input parameters are defined and radiative transfer computations are carried out for all expedient input parameter combinations. The resulting shortwave and longwave radiant flux densities with their appropriate parameter sets are tabulated. Now for every individual input parameter set of each grid cell at each time slice the corresponding radiant flux densities can be derived using multidimensional linear interpolations between the parameter increments.

3 Results

3.1 Comparison with other satellite derived data products

The computed and altitude corrected global radiation at surface over the period of 1984–2000 is based on the highly resolved ISCCP Dx dataset and is shown in Fig. 2

Title Page

Abstract

Introduction

Conclusions

References

Tables

Figures

◀

▶

◀

▶

Back

Close

Full Screen / Esc

Printer-friendly Version

Interactive Discussion

for Central Europe. There the distinctive North-South gradient with values of about 75 W m^{-2} in the North and maxima of 300 W m^{-2} in the South of the investigation area is shown in Fig. 2a. Data gaps along the coastlines are displayed in white. Due to the solely usage of Meteosat data the covered area is limited to the scanned disk so less values above ca. 60° latitude exist. Figure 2b shows the temporal variability of global radiation for the 17 years examined. A statistically firmed increase of global radiation ($10\text{--}20 \text{ W m}^{-2}$) in the South of the target area is distinguished. The strong contours indicate regions with a confidence interval $>99.7\%$ and fine contours assign a confidence interval of $>90.0\text{--}95.0\%$. Positive and negative trends are detected in the remaining Central Europe as well, but they could not be certified.

Additionally the global radiation for the ISCCP D1 and ISCCP D2 datasets was computed using the same look-up table as for the Dx dataset in order to provide a common basis for comparisons between the three datasets. Due to their different temporal and spatial resolutions the datasets are adapted and upscaled to the resolution of the D2 dataset (monthly means, $280 \times 280 \text{ km}^2$). Figure 3 shows that over wide areas the radiant flux densities of the D1 dataset are approx. $10\text{--}15 \text{ W m}^{-2}$ lower than the Dx dataset, except for the most southern area where differences increase up to $20\text{--}30 \text{ W m}^{-2}$. In contrast deviations between the Dx and the D2 dataset only appear in few regions, most notably in alpine regions and in North Africa. Thus values up to $\pm 25 \text{ W m}^{-2}$ in comparison to the Dx dataset can be observed. Considerable discrepancies to the Dx dataset are detected for higher altitudes (Alps) with higher values and for arid environment (North Africa) with lower values for the D1 and D2 dataset. That suggests possible uncertainties in altitude correction and in atmospheric and subjacent surface parameterisation. Given the identical analysis the deviations between the ISCCP D datasets using same method indicate that after adapting to the comparable resolution the parameters of the origin datasets from Dx over D1 to D2 differ considerably. The differences at northern latitudes above 60° are not relevant due to the insufficient Dx data quality as above mentioned.

For verification of the Streamer results the satellite data products of the GEWEX SRB

Long-time global radiation derived from ISCCP Dx data

N. Petrenz et al.

Title Page

Abstract

Introduction

Conclusions

References

Tables

Figures

◀

▶

◀

▶

Back

Close

Full Screen / Esc

Printer-friendly Version

Interactive Discussion

and the ISCCP FD (Rossow and Zhang, 1995) dataset are applied. Both datasets include monthly shortwave and longwave radiant flux densities at TOA and at surface, but on different spatial resolutions. Thus radiative transfer computations for the SRB long time series are carried out on a $1^\circ \times 1^\circ$ global grid on the basis of satellite derived cloud data from the ISCCP Dx dataset. The ISCCP FD data depend on cloud information of the ISCCP D1 dataset on a $2.5^\circ \times 2.5^\circ$ grid.

Hence for comparison the ISCCP Dx and the SRB data are modified and projected onto a grid equivalent to the spatial resolution of the ISCCP FD dataset. The investigation period is 1984–1993 (10 years).

Figures 4b, c clearly present a 25 W m^{-2} higher Dx global radiation at surface for nearly whole Central Europe. In North Africa even values up to 45 W m^{-2} are achieved. Considerable differences for the SRB dataset mainly exist for land surfaces suggesting an incorrect atmospheric parameterisation. The differences to the ISCCP FD dataset are between $5\text{--}20 \text{ W m}^{-2}$. They are distributed over the whole area showing a slight North-South gradient with maxima of 35 W m^{-2} especially over the Mediterranean. These differences were further analysed for special regions, for seasonal cycle as well as the dependence on latitude or longitude within the seasonal cycle, but no sufficient explanation could be found.

3.2 Evaluation with surface measurements

For comparisons with surface measurements data of the “Global Energy Balance Archive” (GEBA) and the “German Meteorological Service” (DWD) are used. The analyses are based on different periods and regions. While the monthly GEBA data are actually available online from January 1983 until December 1990 for 305 stations in Central Europe, the data of the DWD stations exist for the complete investigation period but only for Germany. To evaluate the comparison between satellite derived radiant flux densities and surface measurements complete years and time series are used. Thus the investigation period for the GEBA dataset is 1984 to 1990 (98 Stations, 28 within Germany) and for the DWD dataset the periods are 1984 to 1990 (28 Stations

Long-time global radiation derived from ISCCP Dx data

N. Petrenz et al.

Title Page

Abstract

Introduction

Conclusions

References

Tables

Figures

◀

▶

◀

▶

Back

Close

Full Screen / Esc

Printer-friendly Version

Interactive Discussion

regarding to GEBA) and 1984–2000 (34 Stations).

The results are statistically analysed and presented in Fig. 5. The scatterplot (Fig. 5, left) reflects a good agreement for the global radiation at surface derived from ISCCP Dx data and the values directly measured at the GEBA stations within the corresponding ISCCP Dx pixel ($30 \times 30 \text{ km}^2$). But with increasing global radiation values an increase in scattering is visible. The included statistics for the two datasets reveals that over the whole investigation period the RMSE is 25.8 W m^{-2} and the bias is about 19.4 W m^{-2} . Thus, the values of the ISCCP-Dx pixel are on the average 10% higher than the values directly measured at the ground stations also mirrored in the equation for the best linear fit. The differences range from $5\text{--}25 \text{ W m}^{-2}$.

Other investigations are carried out for Germany using the data of the DWD and GEBA. The scatterplot in Figure 6 illustrates that the Dx global radiation and the DWD global radiation match well, but the Dx data are approx. 12% higher than the DWD data. Outliers are mainly observed for the ISCCP Dx data with tendency to be higher than the pyranometer measurements. The RMSE and the bias between the two datasets are 25.4 W m^{-2} and about 20.6 W m^{-2} respectively. At the individual stations differences from $10\text{--}25 \text{ W m}^{-2}$ occur.

In Fig. 7 analyses regarding observation site measurements of GEBA and DWD are demonstrated. Excluding a few outliers it is apparent that the data show almost no deviations solely the GEBA data are in most instances slightly lower than the DWD data. As expected the surface measurements (GEBA and DWD) agree.

Among the potential reasons for deviations between satellite data and surface measurements, like coarse atmospheric parameterisation within Streamer or changing aerosol contents, the target comparison between a point measurement and an area of $30 \times 30 \text{ km}^2$ is one of the most effective. The individual pixels within this section have a resolution of $4\text{--}7 \text{ km}$. For each time slice one random pixel is used to describe the condition of the whole area. Suboptimal case is that every time an other pixel is chosen to represent a Dx grid cell. Another problem are the radiances determined onboard satellites and in situ because of the different spectral channels of the radiometers. Philipona

Long-time global radiation derived from ISCCP Dx data

N. Petrenz et al.

Title Page

Abstract

Introduction

Conclusions

References

Tables

Figures

◀

▶

◀

▶

Back

Close

Full Screen / Esc

Printer-friendly Version

Interactive Discussion

(2002) assumes in his investigations that unconditioned pyranometer measurements in the past systematically underestimate downward shortwave radiant flux density. After an appropriate correction an approximation of measured and modelled data could be achieved. Generally the uncertainties of surface measurements should be taken into account for validation.

Completing the survey of surface measurements the annual means of global radiation over Germany calculated using the directly measured DWD data (Germany-DWD) and the corresponding ISCCP Dx pixel data (Germany-Dx) over the whole investigation period are compared and analyses of trends are carried out (Fig. 8). Apart from an average difference of 25 W m^{-2} between the two datasets like above mentioned there is a slightly positive trend $< 1.4 \text{ W m}^{-2}$ for the Germany-Dx data but a strong positive trend for the Germany-DWD data of 9.1 W m^{-2} (Fig. 8a) over the period of 1984–2000. Considered separately for each station Figs. 8b, c exhibit irregular positive and negative trends for Germany-Dx and strong positive trends for most Germany-DWD data. Statistically firmed (red circles) is the trend of 10 W m^{-2} of only one Germany-Dx station (Fig. 8b) but there are a number of stations with significant trends for Germany-DWD data. Their trends range between 2 and 20 W m^{-2} . However, it is conspicuously that the firmed station of Germany-Dx is not proved for Germany-DWD.

3.3 Comparison with model data

A further comparison refers to the results of the regional climate models of the respective partners within the project “Quantification of Uncertainties In Regional Climate and Climate Change Simulations” (QUIRCS). The mesoscale hydrostatic “Regional Model” (REMO, Jacob and Podzun, 1997; Jacob, 2001) and the non-hydrostatic “Meteorological Model” (MM5, Grell et al., 1995, 2000) are applied. REMO is used by the BTU Cottbus (BTU, REMO 5.0) as well as by the MPI Hamburg (MPI, REMO 5.1) and MM5 is used by the IMK Karlsruhe. These models operate on a different spatial scale. Hence our results were adapted to the particular available $1/6^\circ$ grid (18 km) of the models. The investigation period of project QUIRCS is 1979–1993 (15 years). Due to the availability

Long-time global radiation derived from ISCCP Dx data

N. Petrenz et al.

Title Page

Abstract

Introduction

Conclusions

References

Tables

Figures

◀

▶

◀

▶

Back

Close

Full Screen / Esc

Printer-friendly Version

Interactive Discussion

of ISCCP D data starting in July 1983 the investigation period is limited to 1984–1993 (10 years). Figure 9 (left) plots the differences of monthly global radiation at surface for Germany simulated by regional climate models with respect to our calculated results. In wintertime the model outputs and our results agree well with mean differences of approx. 12 W m^{-2} and maxima of 25 W m^{-2} but in summertime there are stronger discrepancies between all datasets. Hence the mean annual cycles are examined (Fig. 9, right) and show clearly that our computed global radiation is nearly conform to the results of REMO within the summer months. In winter our results are higher than the model results with values above mentioned. Largest deviations are registered compared to the non-hydrostatic model. Excluding the winter months the MM5 output is obviously lower, on average 30 W m^{-2} .

Detailed analyses for the three German regions Schleswig, Lindenberg and Stuttgart each defined by 49 grid cells show similar results. In Fig. 10 the global radiation at surface with reference to our results (Streamer) is demonstrated. The ten-year means of all models for every region are given in Fig. 10 (right). It becomes obvious that the pattern for each station is always the same, only the range of values is different. Thus our results are all the time the highest and the results of the MM5 are permanent smaller than the remaining model results. Additionally the dependence on the natural North-South gradient of the global radiation is visible. The scatter plot (Fig. 10, left) shows good agreement between Streamer and REMO 5.0 for all stations with a mean RMSE of 15.9 W m^{-2} . Larger variances appear between Streamer and REMO 5.1 as well as for Streamer and MM5. Complete results are shown in Table 2.

4 Discussion and conclusions

The global radiation at surface calculated using look-up tables based on radiative transfer calculations with the 1-D model Streamer are presented in comparison to a number of data products. Our method describes a technique to handle long-time datasets, like ISCCP Dx, with high temporal and spatial resolution. Uncertainties that become appar-

Long-time global radiation derived from ISCCP Dx data

N. Petrenz et al.

Title Page

Abstract

Introduction

Conclusions

References

Tables

Figures

◀

▶

◀

▶

Back

Close

Full Screen / Esc

Printer-friendly Version

Interactive Discussion

ent in the evaluation with other datasets are caused by assumptions and simplifications using defined constants and increments for the look-up tables to determine the short-wave and longwave radiant flux densities at TOA and at surface. Also data gaps and systematic gaps in the ISCCP Dx dataset intensify these uncertainties.

In general the global radiation exhibits on average higher values over the whole investigation area as well as for special regions than the products of comparison. Thus the comparison between the satellite data based products reveal mostly higher values with differences of $5\text{--}45\text{ W m}^{-2}$ to the SRB dataset and -35 W m^{-2} to the ISCCP FD dataset.

Surface measurements of global radiation for all available stations in Central Europe and in Germany reveal RMSEs of ca. 26 W m^{-2} in relation to our data and biases of ca. 20 W m^{-2} that cause a 10–12% higher amount of global radiation at surface for our method. The comparison between surface measurements shows only small differences while the comparison of point measurement to area measurement is more difficult. In addition the atmospheric parameterisation for Streamer seems to be too coarse.

Consequently improvements for the look-up tables are planned enabling the variable integration of additional atmospheric parameters and conditions. As next step a better solution for replacing the gaps of the original ISCCP datasets and therefore reducing associated uncertainties are sought at present.

In spite of the demonstrated problems according to the data basis and the used method the attained results are valuable because of their highly resolved spatial area-integrated information over a long investigation period. The produced radiant flux density datasets and especially the revised datasets are a solid basis for further improvements and investigations.

Acknowledgements. The presented study was part of the research project Quantification of Uncertainties In Regional Climate and Climate Change Simulations (QUIRCS), funded within the German Climate Research Program (DEKLIM). We thank the NASA Langley Research Center Atmospheric Sciences Data Center for providing the ISCCP D data as well as the ISCCP

Long-time global radiation derived from ISCCP Dx data

N. Petrenz et al.

Title Page

Abstract

Introduction

Conclusions

References

Tables

Figures

◀

▶

◀

▶

Back

Close

Full Screen / Esc

Printer-friendly Version

Interactive Discussion

FD and GEWEX SRB data. The surface radiation data (GEBA, DWD data) have been kindly provided by the ETH Zurich and the German Meteorological Service. We thank J. Key for providing the RTM Streamer. The authors wish to thank all involved persons for their help and for supplying model results.

5 **References**

Augustine, J. A., DeLuisi, J. J., and Long, C. N.: SURFRAD – A National Surface Radiation Budget Network for Atmospheric research, Bull. Amer. Meteorol. Soc., 81, 2341–2357, 2000.

10 Barkstrom, B., Harrison, E., Smith, G., Green, R., Kibler, J., Cess, R., and the ERBE Science Team: Earth Radiation Budget Experiment (ERBE) archival and April 1985 results, Bull. Amer. Meteorol. Soc., 70, 1254–1262, 1989.

Darnell, W. L., Staylor, W. F., Gupta, S. K., and Denn, F. M.: Estimation of Surface Insolation using sun-synchronous Satellite data, J. Climate, 1, 820–835, 1988.

15 Darnell, W. L., Staylor, W. F., Gupta, S. K., Ritchey, N. A., and Wilber, A. C.: Seasonal variation of surface radiation budget derived from International Satellite Cloud Climatology Project C1 data, J. Geophys. Res., 97, 15 741–15 760, 1992.

Jacob, D. and Podzun, R.: Sensitivity studies with the regional climate model REMO, Meteorol. Atmos. Phys., 63, 119–129, 1997.

Jacob, D.: A note to the simulation of the annual and inter-annual variability of the water budget over the Baltic Sea drainage basin, Meteorol. Atmos. Phys., 77, 61–73, 2001.

20 Gilgen, H., Wild, M., and Ohmura, A.: Global Energy Balance Archive (GEBA) Report 3: The GEBA Version 1995 Database, Zürcher Geographische Schriften 74, 105 pp. (available from Institute of Geography ETH, Winterthurerstr. 190, CH-8057 Zurich, Switzerland), 1997.

Gilgen, H. and Ohmura, A.: The Global Energy Balance Archive (GEBA), Bull. Amer. Meteorol. Soc., 80, 831–850, 1999.

25 Grell, G. A., Dudhia, J., and Stauffer, D. R.: A description of the fifth generation Penn State/NCAR mesoscale model (MM5), Technical report, National Centre for Atmospheric Research, Boulder, Colorado, USA, NCAR/TN-398+STR, 1995.

Grell, G. A., Schade, L., Knoche, R., Pfeiffer, A., and Egger, J.: Nonhydrostatic climate simulations over complex terrain, J. Geophys. Res., 105(D4), 29 595–29 608, 2000.

30

Long-time global radiation derived from ISCCP Dx data

N. Petrenz et al.

Title Page	
Abstract	Introduction
Conclusions	References
Tables	Figures
◀◀	▶▶
◀	▶
Back	Close
Full Screen / Esc	
Printer-friendly Version	
Interactive Discussion	

- Gupta, S. K., Darnell, W. L., and Wilber, A. C.: A Parametrization for Longwave Surface Radiation from Satellite Data: Recent Improvements, *J. Appl. Meteorol.*, 31, 1361–1367, 1992.
- Hollmann, R., Müller, R. W., and Gratzki, A.: CM-SAF surface radiation budget: First results with AVHRR data, *Adv. Space Res.*, 37, 2166–2171, doi:10.1016/j.asr.2005.10.044, 2006.
- 5 Key, J. R.: Streamer – User's Guide, NOAA/NESDIS, 70pp., 2001.
- McMillin, L. M.: Evaluation of a Classification Method for Retrieving Atmospheric Temperatures from Satellite Measurements, *J. Appl. Meteorol.*, 30, 432–446, 1991.
- Ohmura, A., Dutton, E. G., Forgan, B., and Co-Authors: Baseline Surface Radiation Network (BSRN/WCRP): New Precision Radiometry for Climate Research, *Bull. Amer. Meteorol. Soc.*, 79, 2115–2136, 1998.
- 10 Pinker, R. T. and Laszlo, I.: Modeling Surface Solar Irradiance for Satellite Applications on a Global Scale, *J. Appl. Meteorol.*, 31, 194–211, 1992.
- Pinker, R. T., Frouin, R., and Li, Z.: A Review of Satellite Methods to Derive Surface Short-wave Irradiance, *Rem. Sens. Environ.*, 51, 108–124, 1995.
- 15 PRFI: Polar Radiation Fluxes from ISCCP (PRFI) – Procedure Description, <http://stratus.ssec.wisc.edu/products/d1fluxes/fluxes3.html>, 2000.
- Rapp, J.: Konzeption, Problematik und Ergebnisse klimatologischer Trends für Europa und Deutschland, *Berichte des Deutschen Wetterdienstes* 212, Offenbach am Main, Selbstverlag des Deutschen Wetterdienstes, 2000.
- 20 Raschke, E., Ohmura, A., Rossow, W. B., Carlson, B. E., Zhang, Y. C., Stubenrauch, C., Kottek, M., and Wild, M.: Cloud Effects on the Radiation Budget Based on ISCCP Data (1991 to 1995), *Int. J. Climatol.*, 25, 1103–1125, 2005.
- Raschke, E., Bakan, S., and Kinne, S.: An assessment of radiation budget data provided by the ISCCP and GEWEX-SRB, *Geophys. Res. Lett.*, 33, L07812, doi:10.1029/2005GL025503, 2006.
- 25 Rossow, W. B. and Schiffer, R. A.: ISCCP Cloud data Products, *Bull. Amer. Meteorol. Soc.*, 72, 2–20, 1991.
- Rossow, W. B., Garder, L. C., Lu, P. J., and Walker, A. W.: International Satellite Cloud Climatology Project (ISCCP) Documentation of Cloud Data, WMO/TD-266, (revised), 76pp. plus three appendices, *World Clim. Res. Progr. (ICSU and WMO)*, Geneva, March, 1991.
- 30 Rossow, W. B. and Zhang, Y. C.: Calculation of Surface and Top of Atmosphere Radiative Fluxes from Physical Quantities Based on ISCCP Data Sets, 2. Validation and first results, *J. Geophys. Res.*, 100, 1167–1197, 1995.

Long-time global radiation derived from ISCCP Dx data

N. Petrenz et al.

Title Page

Abstract

Introduction

Conclusions

References

Tables

Figures

◀

▶

◀

▶

Back

Close

Full Screen / Esc

Printer-friendly Version

Interactive Discussion

- Rossow, W. B. and Zhang, Y. C.: Documentation of Radiative Flux Dataset (FC), http://isccp.giss.nasa.gov/docs/docs_fc.html, 1995.
- Rossow, W. B., Walker, A. W., Beuschel, D. E., and Roiter, M. D.: International Satellite Cloud Climatology Project (ISCCP): Documentation of new cloud Datasets, WMO/TD-No. 737, World climate research Programme (ICSU and WMO), Genf, 1996.
- Rossow, W. B. and Schiffer, R. A.: Advances in Understanding Clouds from ISCCP, Bull. Amer. Meteorol. Soc., 80, 2261–2287, 1999.
- Schiffer, R. A. and Rossow, W. B.: The International Satellite Cloud Climatology Project (ISCCP): The first project of the World Climate Research Programme, Bull. Amer. Meteorol. Soc., 64, 779–984, 1983.
- Stackhouse, P. W., Gupta, S. K., Cox, S. J., Chiacchio, M., and Mikovitz, J. C.: The WCRP/GEWEX Surface Radiation Budget Project Release 2: An assessment of surface fluxes at 1 degree resolution, 2000, in: Current Problems in Atmospheric Radiation, International Radiation Symposium, IRS 2000, edited by: Smith, W. L. and Timofeyev, Y. M., St. Petersburg, Russia, 24–29 July 2000.
- Stamnes, K., Tsay S. C., Wiscombe, W., and Jayaweera, K.: Numerically Stable Algorithm for Discrete-Ordinate-Method Radiative Transfer in Multiple Scattering and Emitting Layered Media, Appl. Opt., 27, 2502–2509, 1988.
- Stokes, G. M. and Schwartz, S. E.: The Atmospheric Radiation Measurement (ARM) Program: Programmatic and Design of the Cloud and Radiation Test Bed, Bull. Amer. Meteorol. Soc., 75, 1201–1221, 1994.
- Toon, O. B., McKay, C. P., and Ackermann, T. P.: Rapid Calculation of Radiative Heating Rates and Photodissociation Rates in Inhomogeneous Multiple Scattering Atmospheres, J. Geophys. Res., 94, 16 287–16 301, 1989.
- Wielicki, B. A., Barkstrom, B. R., Harrison, E. F., and Co-Authors: Clouds and the Earth's Radiant Energy System (CERES): Algorithm Overview, IEEE Transactions on Geoscience and Remote Sensing, 36, 1127–1141, 1998.
- Zhang, Y. C., Rossow, W. B., and Lacis, A. A.: Calculation of Surface and Top of Atmosphere Radiative Fluxes from Physical Quantities Based on ISCCP Data Sets, 1. Method and Sensitivity to Input data Uncertainties, J. Geophys. Res., 100, 1149–1165, 1995.

Long-time global radiation derived from ISCCP Dx data

N. Petrenz et al.

Title Page

Abstract

Introduction

Conclusions

References

Tables

Figures

◀

▶

◀

▶

Back

Close

Full Screen / Esc

Printer-friendly Version

Interactive Discussion

Long-time global radiation derived from ISCCP Dx data

N. Petrenz et al.

Table 1. Summary of the used ISCCP data products according to Rossow et al. (1996).

Dataset	Temporal Resolution	Spatial Resolution	Parameters Cloud	Surface	Other
ISCCP Dx	3-hourly	ca. 30×30 km ²	– cloud top temperature – cloud top pressure – optical thickness	– (clear sky) surface temperature – land/water/ near shore flag – snow/ice code	– latitude, longitude – solar zenith angle – day/night flag
ISCCP D1	3-hourly	ca. 280×280 km ²	– cloud top temperature – cloud top pressure – optical thickness	– (clear sky) surface temperature – land/water cover – snow/ice cover	– latitude, longitude – solar zenith angle – day/night
ISCCP D2	3-hourly monthly means	ca. 280×280 km ²	– cloud top temperature – cloud top pressure – optical thickness	– surface temperature – land/water cover – snow/ice cover	– latitude, longitude

Title Page

Abstract

Introduction

Conclusions

References

Tables

Figures

◀

▶

◀

▶

Back

Close

Full Screen / Esc

Printer-friendly Version

Interactive Discussion

Long-time global radiation derived from ISCCP Dx data

N. Petrenz et al.

Table 2. Summary of statistical values of global radiation at surface with reference to the TUD dataset based on the ISCCP Dx data and the RTM Streamer (S) in comparison to the results of the regional climate models REMO 5.0 (BTU), REMO 5.1 (MPI), MM5 (IFU) for the German regions Schleswig, Lindenberg and Stuttgart over the period of 1984–1993.

	Schleswig			Lindenberg			Stuttgart		
	S-REMO 5.0	S-REMO 5.1	S-MM5	S-REMO 5.0	S-REMO 5.1	S-MM5	S-REMO 5.0	S-REMO 5.1	S-MM5
Mean [W m ⁻²]	121.5	122.2	106.5	130.7	132.4	117.1	142.9	144.7	133.4
Bias [W m ⁻²]	8.2	4.8	35.4	8.5	7.2	38.5	8.5	5.0	27.6
RMSE [W m ⁻²]	16.0	19.1	45.7	17.3	22.4	40.9	14.3	17.4	30.9
R ²	0.97	0.95	0.95	0.98	0.96	0.94	0.98	0.97	0.98
N	120	120	120	120	120	120	120	120	120

[Title Page](#)
[Abstract](#)
[Introduction](#)
[Conclusions](#)
[References](#)
[Tables](#)
[Figures](#)
[I◀](#)
[▶I](#)
[◀](#)
[▶](#)
[Back](#)
[Close](#)
[Full Screen / Esc](#)
[Printer-friendly Version](#)
[Interactive Discussion](#)

**Long-time global
radiation derived
from ISCCP Dx data**

N. Petrenz et al.

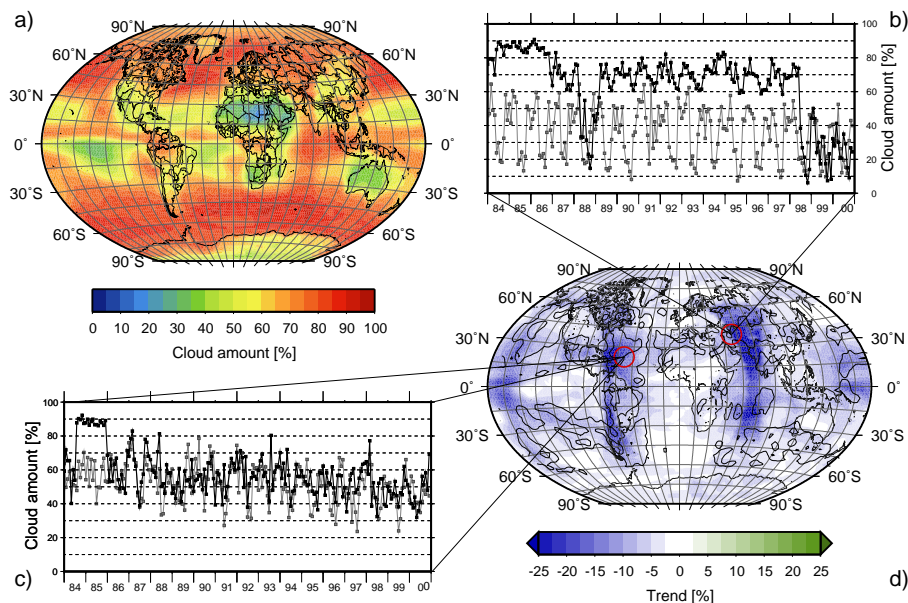


Fig. 1. Mean global ISCCP D1 cloud amount. **(a)** Annual mean over the period of 1984–2000. **(d)** Significant temporal variances within black contoured regions over the periods of 1984–2000. **(b), (c)** Obvious inhomogeneities of time series in two special regions (inhomogeneous time series are black).

Title Page

Abstract

Introduction

Conclusions

References

Tables

Figures

◀

▶

◀

▶

Back

Close

Full Screen / Esc

Printer-friendly Version

Interactive Discussion

**Long-time global
radiation derived
from ISCCP Dx data**

N. Petrenz et al.

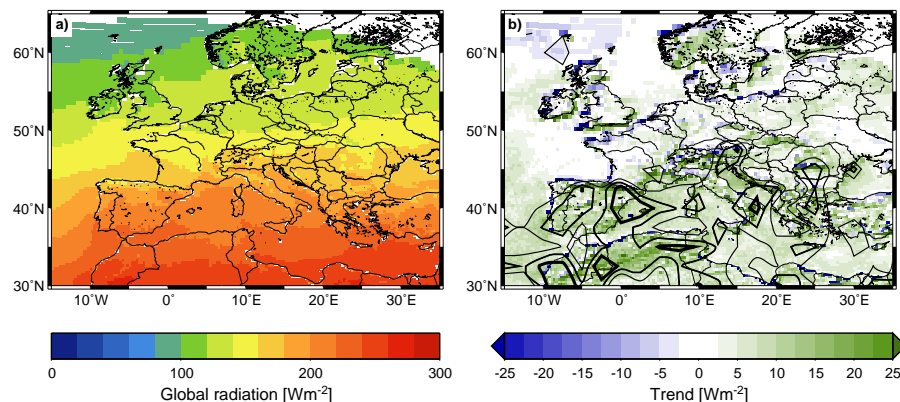


Fig. 2. Global radiation at surface based on ISCCP Dx data. **(a)** Annual mean over the period of 1984–2000, **(b)** Temporal trend over the period of 1984–2000 with areas of statistical significance (black contoured).

[Title Page](#)[Abstract](#)[Introduction](#)[Conclusions](#)[References](#)[Tables](#)[Figures](#)[◀](#)[▶](#)[◀](#)[▶](#)[Back](#)[Close](#)[Full Screen / Esc](#)[Printer-friendly Version](#)[Interactive Discussion](#)

**Long-time global
radiation derived
from ISCCP Dx data**

N. Petrenz et al.

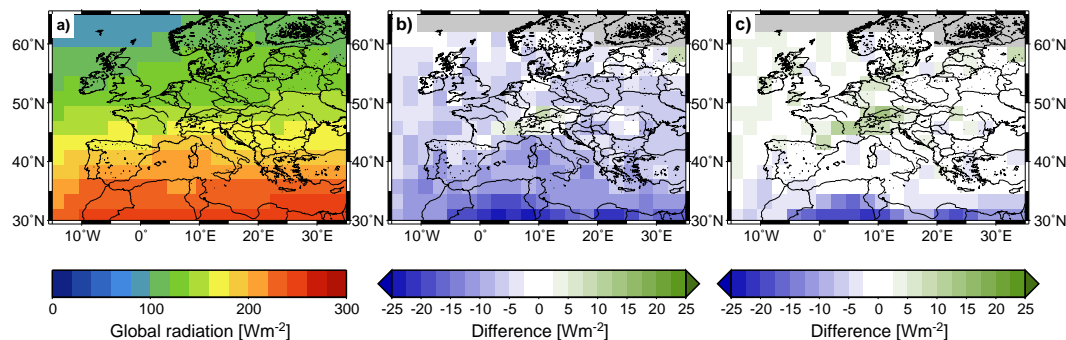


Fig. 3. Comparison of calculated global radiation at surface over the period of 1984–2000. **(a)** ISCCP Dx dataset (reference) and the appropriate differences to the ISCCP D1 dataset **(b):** D1-Dx) as well as to the ISCCP D2 dataset **(c: D2-Dx).**

[Title Page](#)[Abstract](#)[Introduction](#)[Conclusions](#)[References](#)[Tables](#)[Figures](#)[◀](#)[▶](#)[◀](#)[▶](#)[Back](#)[Close](#)[Full Screen / Esc](#)[Printer-friendly Version](#)[Interactive Discussion](#)

**Long-time global
radiation derived
from ISCCP Dx data**

N. Petrenz et al.

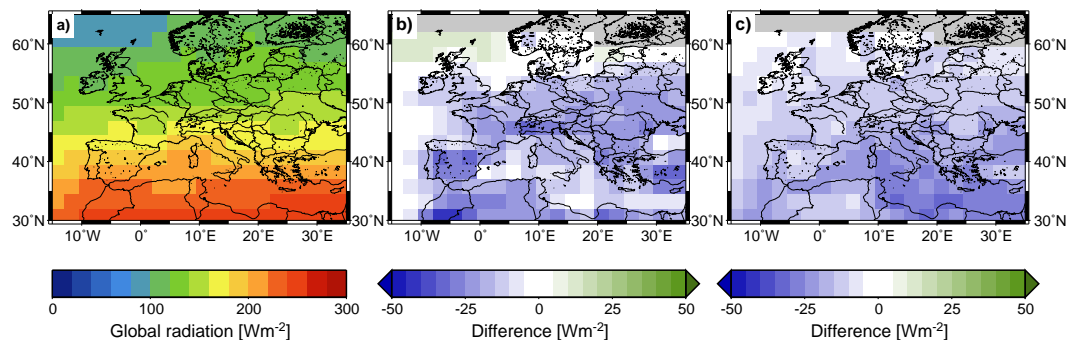


Fig. 4. Comparison of calculated global radiation at surface over the period of 1984–1993; **(a)** ISCCP Dx dataset (reference) and the appropriate differences to the GEWEX SRB dataset **(b)**: SRB-Dx) as well as to the ISCCP FD dataset **(c)**: FD-Dx).

[Title Page](#)[Abstract](#)[Introduction](#)[Conclusions](#)[References](#)[Tables](#)[Figures](#)[◀](#)[▶](#)[◀](#)[▶](#)[Back](#)[Close](#)[Full Screen / Esc](#)[Printer-friendly Version](#)[Interactive Discussion](#)

**Long-time global
radiation derived
from ISCCP Dx data**

N. Petrenz et al.

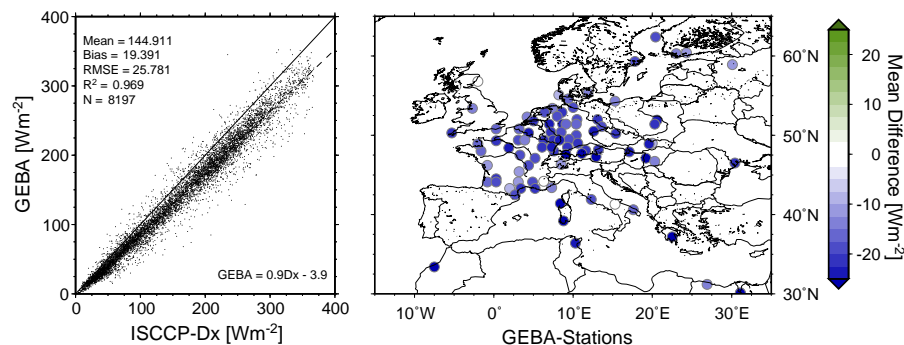


Fig. 5. Monthly global radiation at surface over the period of 1984–1990 for the ISCCP Dx data in comparison with all available GEBA-Stations of Central Europe (left) and the mean difference at each station between the Dx and GEBA data (right, Dx-GEBA).

Title Page

Abstract

Introduction

Conclusions

References

Tables

Figures

◀

▶

◀

▶

Back

Close

Full Screen / Esc

Printer-friendly Version

Interactive Discussion

**Long-time global
radiation derived
from ISCCP Dx data**

N. Petrenz et al.

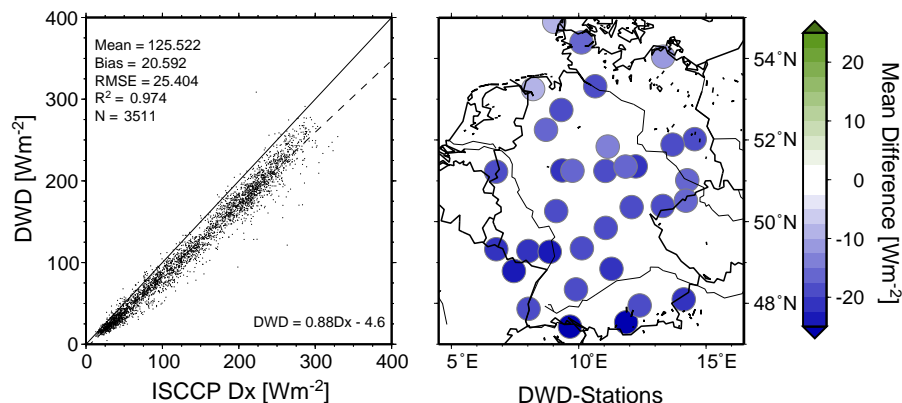


Fig. 6. Monthly global radiation at surface over the period of 1984–1990 for the ISCCP Dx data in comparison with the DWD data of all available gauging stations within the meteorological network of Germany (left) and the mean differences at each station between the Dx and DWD data (right, Dx-DWD).

[Title Page](#)[Abstract](#)[Introduction](#)[Conclusions](#)[References](#)[Tables](#)[Figures](#)[◀](#)[▶](#)[◀](#)[▶](#)[Back](#)[Close](#)[Full Screen / Esc](#)[Printer-friendly Version](#)[Interactive Discussion](#)

**Long-time global
radiation derived
from ISCCP Dx data**

N. Petrenz et al.

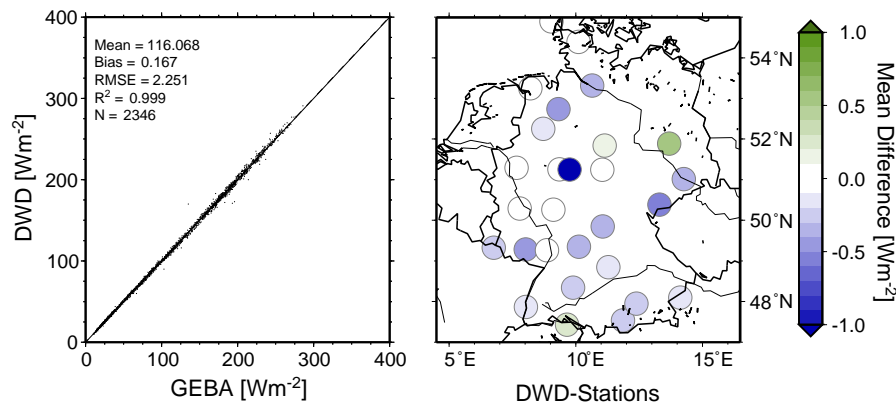


Fig. 7. Monthly global radiation at surface over the period of 1984–1990 for the GEBA data in comparison to the DWD data of all available GEBA stations within the meteorological network of Germany (left) and the mean differences at each station between the GEBA and DWD data (right, GEBA–DWD).

[Title Page](#)[Abstract](#)[Introduction](#)[Conclusions](#)[References](#)[Tables](#)[Figures](#)[◀](#)[▶](#)[◀](#)[▶](#)[Back](#)[Close](#)[Full Screen / Esc](#)[Printer-friendly Version](#)[Interactive Discussion](#)

**Long-time global
radiation derived
from ISCCP Dx data**

N. Petrenz et al.

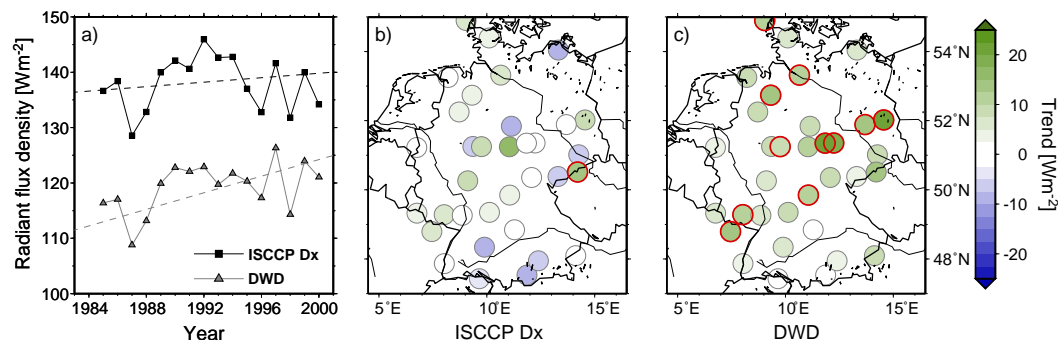


Fig. 8. (a) Annual station means of global radiation at surface over the period of 1984–2000 for the ISCCP Dx data and the DWD data of all available gauging stations within the meteorological network of Germany, (b), (c) temporal trends over the period of 1984–2000 with statistical significant stations (red circles).

[Title Page](#)[Abstract](#)[Introduction](#)[Conclusions](#)[References](#)[Tables](#)[Figures](#)[◀](#)[▶](#)[◀](#)[▶](#)[Back](#)[Close](#)[Full Screen / Esc](#)[Printer-friendly Version](#)[Interactive Discussion](#)

Long-time global radiation derived from ISCCP Dx data

N. Petrenz et al.

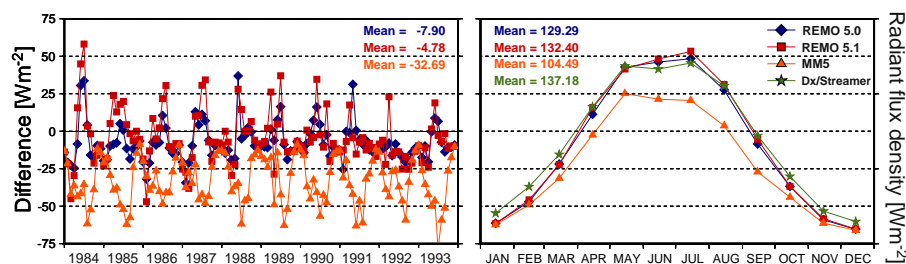


Fig. 9. Monthly differences of global radiation at surface over Germany between the ISCCP Dx data and the results of the regional climate models of the project partners (left: model-Dx) in comparison with the monthly means (right: REMO 5.0 – BTU, blue; REMO 5.1 – MPI, red; MM5 – IFU, orange; Dx/Streamer, green) over the period of 1984–1993.

[Title Page](#)[Abstract](#)[Introduction](#)[Conclusions](#)[References](#)[Tables](#)[Figures](#)[◀](#)[▶](#)[◀](#)[▶](#)[Back](#)[Close](#)[Full Screen / Esc](#)[Printer-friendly Version](#)[Interactive Discussion](#)

Long-time global radiation derived from ISCCP Dx data

N. Petrenz et al.

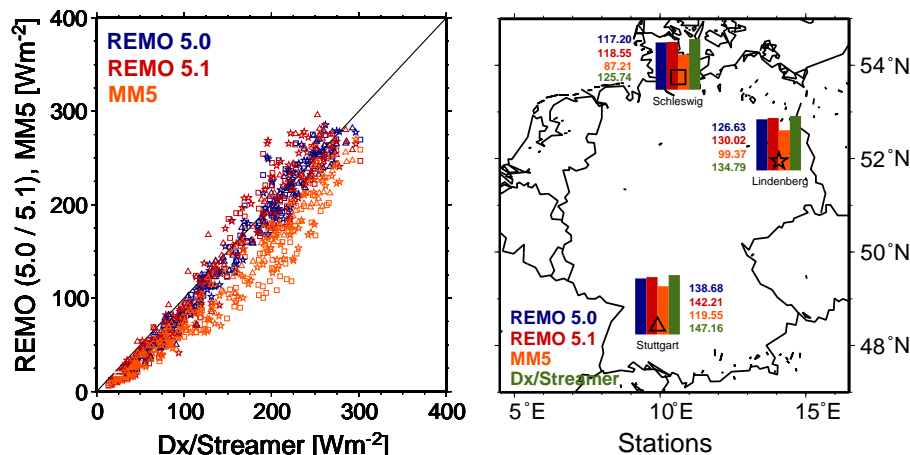


Fig. 10. Comparison of global radiation at surface (left: monthly values; right: 10-year means) for the regions Schleswig, Lindenberg and Stuttgart based on ISCCP Dx data (Dx/Streamer, green) and on the results of the regional climate models of the project partners (REMO 5.0 – BTU, blue; REMO 5.1 – MPI, red; MM5 – IFU, orange) over the period of 1984–1993.

Title Page

Abstract

Introduction

Conclusions

References

Tables

Figures

◀

▶

◀

▶

Back

Close

Full Screen / Esc

Printer-friendly Version

Interactive Discussion